

Supporting Information (SI):

Water splitting cycle for hydrogen production at photo-induced oxygen vacancies using solar energy: experiments and DFT calculation on pure and metal-doped CeO₂

Rui Li^{a,b}, *Chang Wen*^{a,b,c*}, *Kai Yan*^a, *Tianyu Liu*^c, *Bohan Zhang*^b, *Mingtao Xu*^b,
Zijian Zhou^c

^a China-EU Institute for Clean and Renewable Energy, Huazhong University of Science and Technology, Wuhan 430074, China;

^b Department of New Energy Science and Engineering, School of Energy and Power Engineering, Huazhong University of Science and Technology, Wuhan 430074, China;

^c State Key Laboratory of Coal Combustion, School of Energy and Power Engineering, Huazhong University of Science and Technology, Wuhan 430074, China.

*CORRESPONDING AUTHOR:

Chang Wen. Email: wenchang@hust.edu.cn.

Tel: +86-27-87544779, Fax: +86-27-87545526.

Mailing address: School of Energy and Power Engineering, Huazhong University of Science and Technology, 1037 Luoyu Road, Wuhan 430074, China.

Including 13 Figures, 2 Tables.

1. Lists of materials for fabrication

CeO₂ purchased from Aladdin (Ar, 99.5%).

Iron (III) nitrate nonahydrate (Fe(NO₃)₃) purchased from Macklin (Ar, 99%).

Cerium nitrate hexahydrate (Ce(NO₃)₃) purchased from Macklin (Ar, 99%).

Chromium (III) nitrate nonahydrate (Cr(NO₃)₃) purchased from Aladdin (Ar, 98.5%).

Cobalt nitrate hexahydrate (Co(NO₃)₂) from Aladdin (Ar, 99%).

Zirconium (IV) oxynitrate hydrate (Zr(NO₃)₂) from Aladdin (Ar, 99.5%).

Zinc nitrate hexahydrate (Zn(NO₃)₂) from Aladdin (Ar, 99%).

Copper nitrate hydrate (Cu(NO₃)₂) from Aladdin (Ar, 99%).

Samarium(III) nitrate hexahydrate (Sm(NO₃)₃) from chronchem (Ar, 99%).

Lanthanum nitrate hexahydrate (La(NO₃)₃) from Aladdin (Ar, 99%).

Neodymium nitrate hexahydrate (Nd(NO₃)₃) from chronchem (Ar, 99%).

Table S1. The experimental and calculated doping ratio

| Doped element | Calculated ratio (%) | Experimental ratio (%) |
|---------------|----------------------|------------------------|
| Sm | 10 | 9.5 |
| Nd | 10 | 7.9 |
| La | 10 | 10.6 |
| Zn | 10 | 11.8 |
| Zr | 10 | 10.7 |
| Cu | 10 | 9.7 |
| Fe | 10 | 8.0 |
| Cr | 10 | 10.8 |
| Co | 10 | 9.9 |

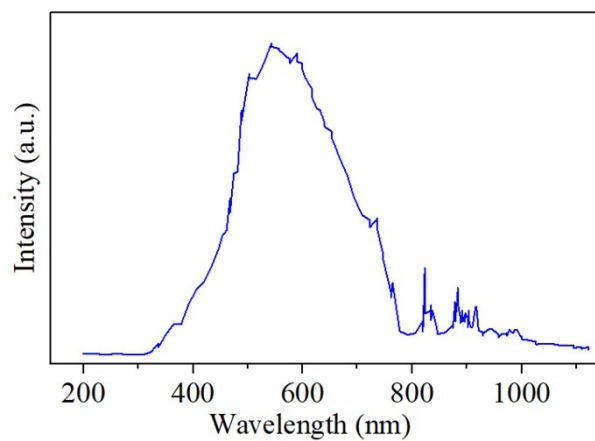


Fig. S1. Spectrum of 300W Xenon lamp.

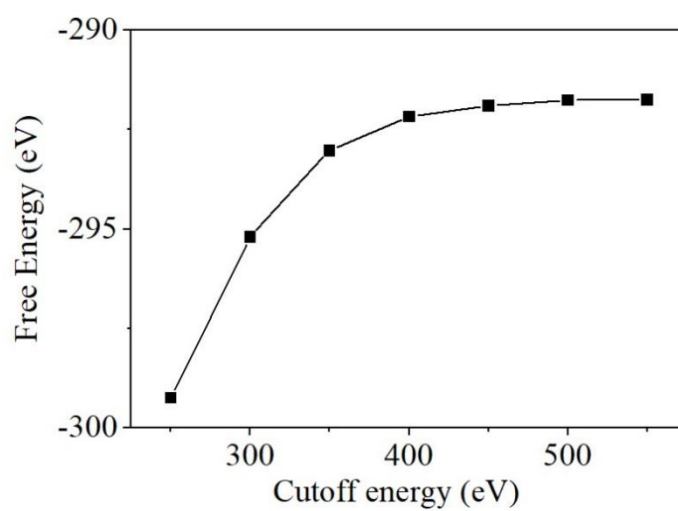


Fig. S2. Correlation between free energy and cutoff energy

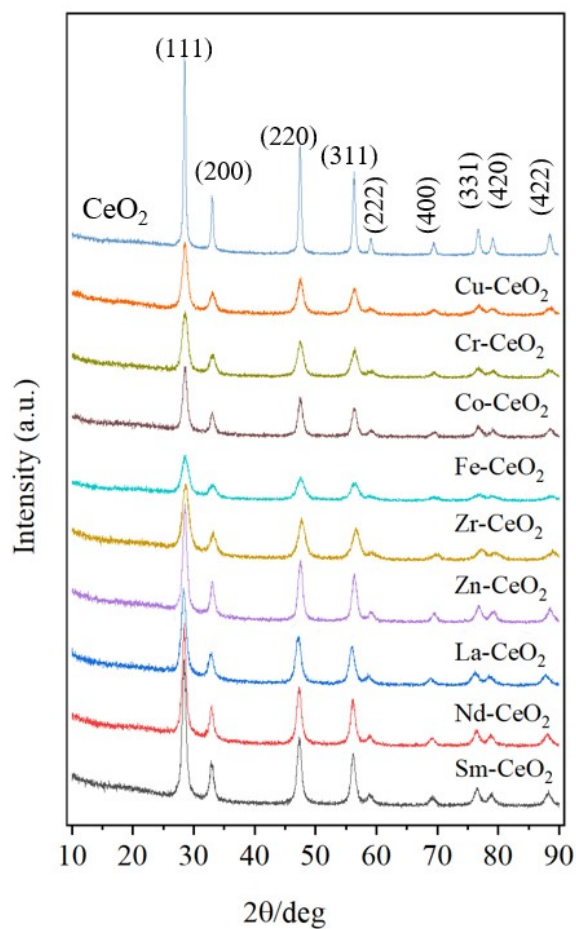


Fig. S3. XRD patterns of pure CeO₂ and metal-doped CeO₂.

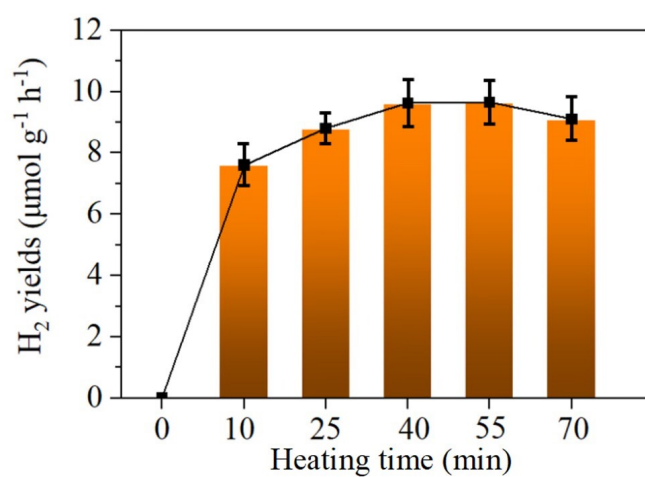


Fig. S4. H₂ yields by CeO₂ in individual PTC experiments with different heating time.

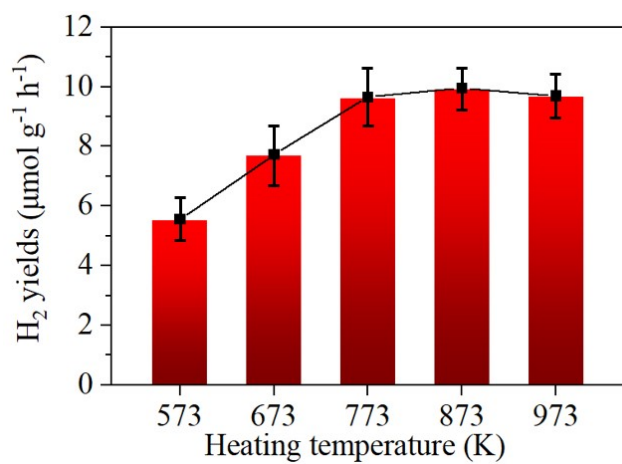


Fig. S5. H₂ yields by CeO₂ in individual PTC experiments with different heating temperature.

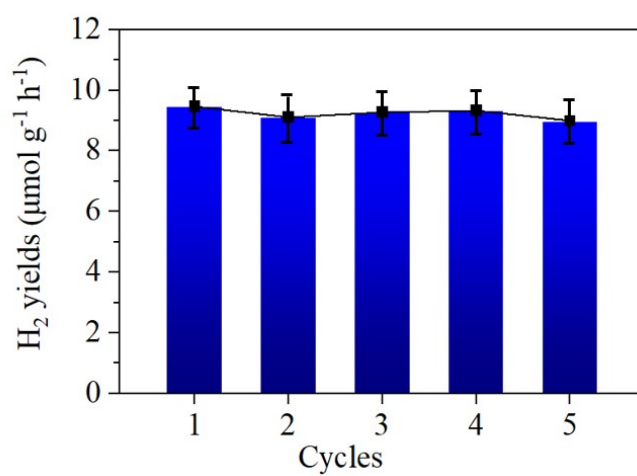


Fig. S6. H₂ yields by CeO₂ in five consecutive cycles of the PTC experiments (irradiation time:

40 min, heating time: 40 min, heating temperature: 773 K).

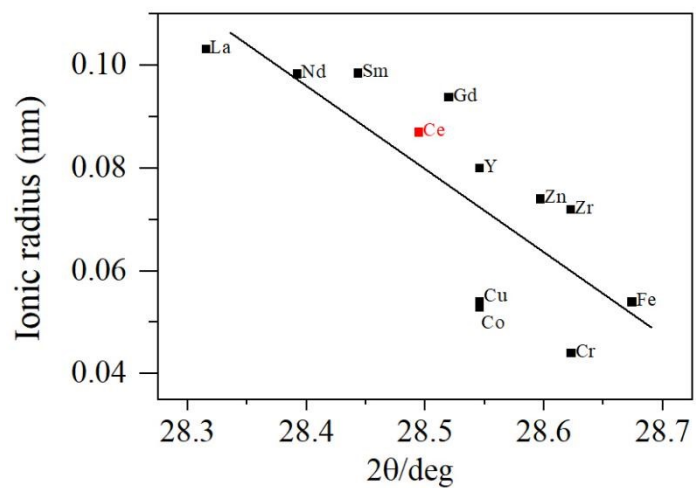


Fig. S7. The relationship between the (111) plane shifts and the ion radius of dopants.

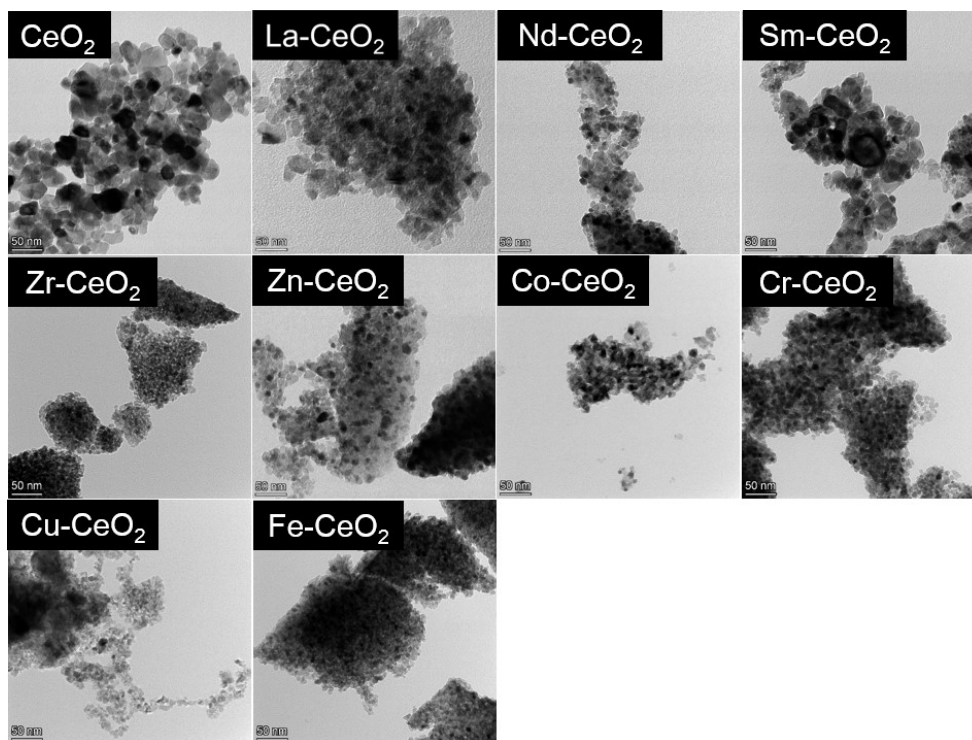


Fig. S8. TEM images of pure CeO_2 and metal-doped CeO_2 .

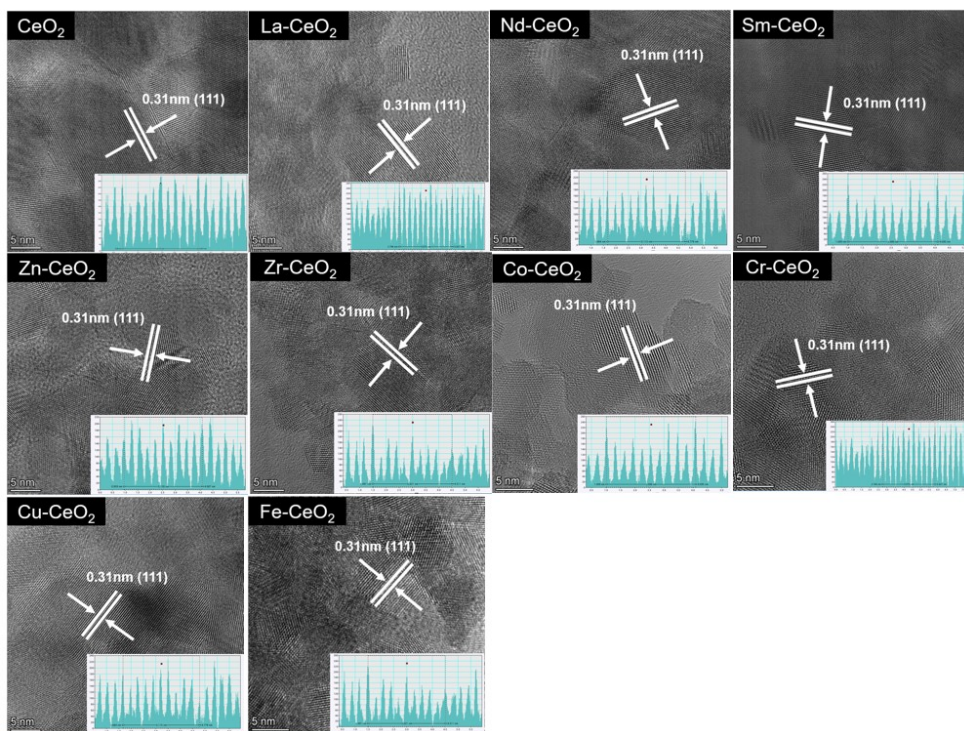


Fig. S9. TEM images of pure CeO_2 and metal ions doped CeO_2 .

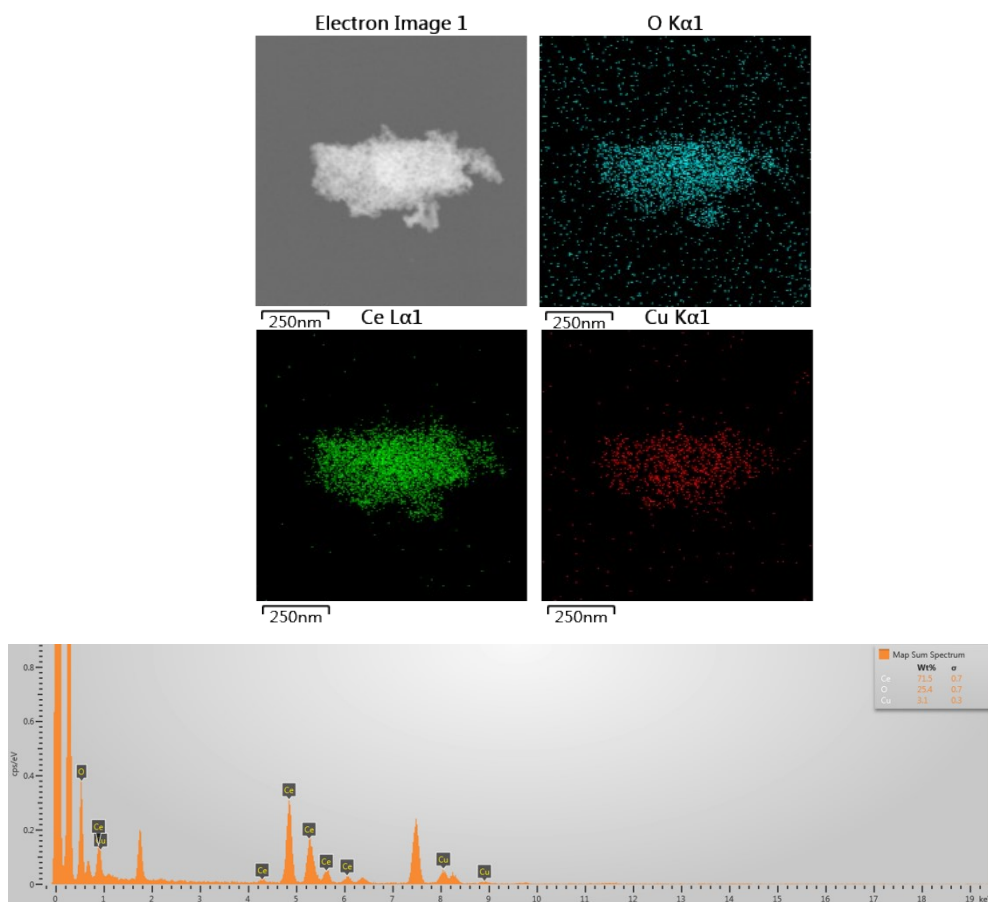


Fig. S10. EDS mapping of Cu-CeO_2 .

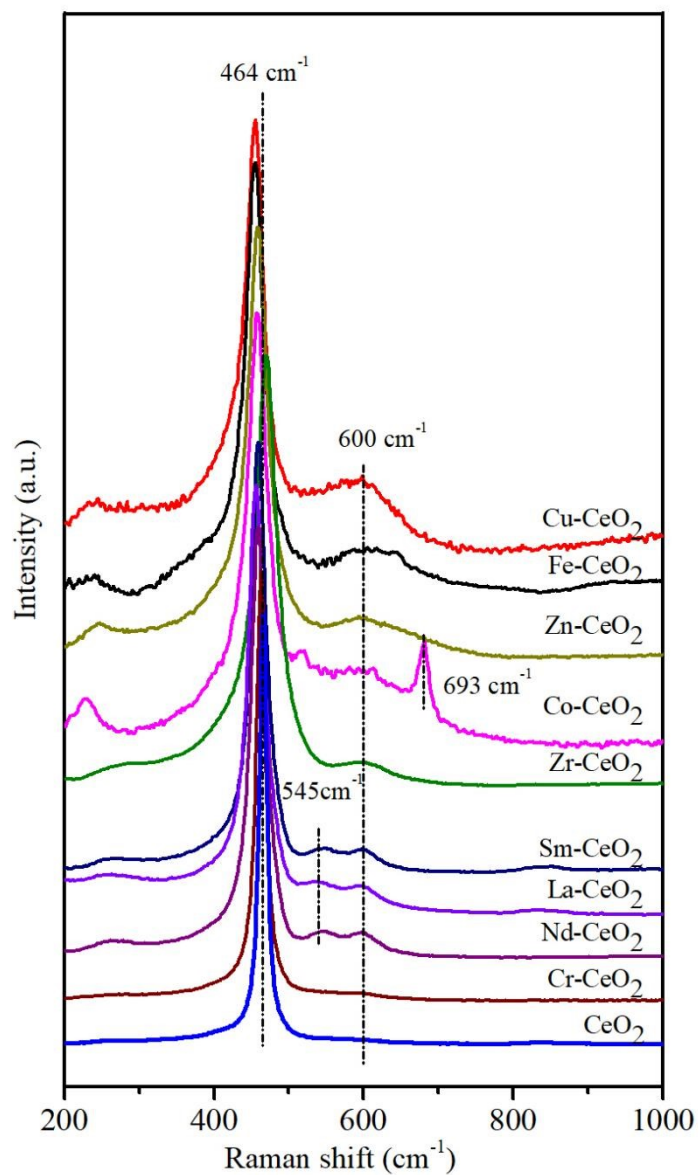


Fig. S11. Raman spectra of CeO₂ and metal ions doped CeO₂.

Table S2. The element ratio of Cu-TiO₂ obtained by EDS

| Elements | Wt% | At% |
|----------|------|-------|
| O | 25.1 | 73.31 |
| Cu | 3.86 | 2.81 |
| Ce | 71.5 | 23.86 |

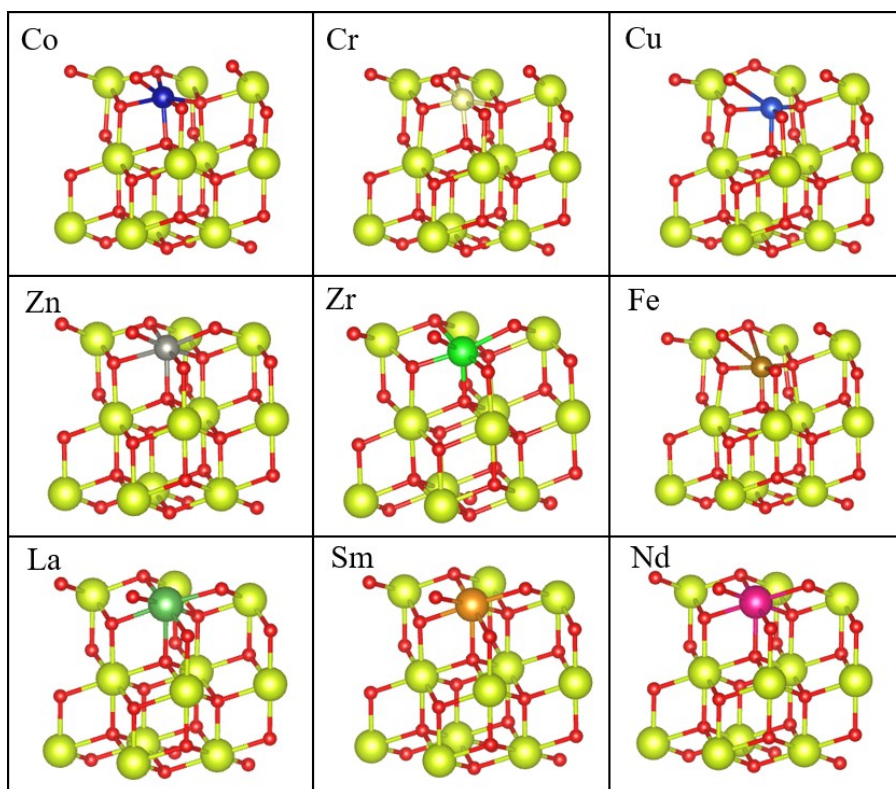


Fig. S12. Models of metal-doped CeO₂ presenting lattice distortion.

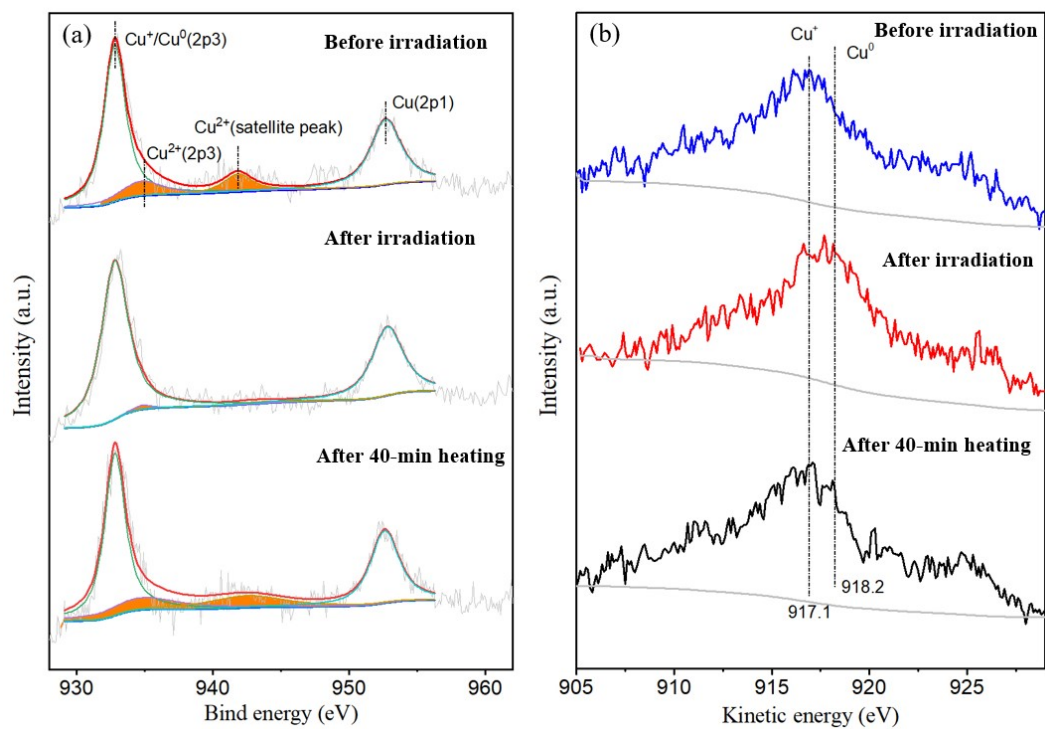


Fig. S13. (a) Cu-2p XPS spectra of the Cu-CeO₂; (b) Auger spectra of Cu LMM.